An Investigation into Near-UV Hydrosilylation of Freestanding Silicon Nanocrystals

Joel A. Kelly and Jonathan G. C. Veinot*

Department of Chemistry, University of Alberta, Edmonton Alberta T6G 2G2, Canada

ARTICLE

ABSTRACT We present a study of the photochemical hydrosilylation of freestanding silicon nanocrystals (Si-NCs) using a near-UV source. The impact of reaction with alkenes and alkynes was studied using *in situ* photoluminescence (PL) spectroscopy, allowing measurement of both changes in intensity and PL maxima during the reaction. Understanding this behavior is important for the utilization of these materials in a number of applications where hydrosilylation is a leading method to functionalize Si-NCs. Changes in the PL were studied and shown arise from the influence of oxidation as well as the Si—C bond formation. Hydrosilylation with a range of conjugated alkynyl species was studied to understand how the introduction of these species to the NC surface can quench the PL from Si-NCs. These results were explained in context of the free-radical and exciton-mediated mechanisms for photochemical hydrosilylation proposed for Si-NCs. Materials in this study were characterized by Fourier transform infrared spectroscopy (FTIR), high-resolution transmission electron microscopy (HRTEM), selected electron area diffraction (SAED), energy dispersive X-ray spectroscopy (EDS), thermogravimetric analysis (TGA) and dynamic light scattering (DLS).

KEYWORDS: silicon nanocrystals · photoluminescence · photochemical hydrosilylation · functionalization

Nanostructured silicon exhibits fascinating size-dependent electronic and optical properties. Efficient photoluminescence (PL) in the visible and near-IR spectral regions has generated tremendous interest in the synthesis and characterization of these materials for a range of applications.[1−3] In particular, concerns regarding the cytotoxicity of compound semiconductor nanocrystals (NCs) (*e.g.*, CdSe, GaAs) for *in vivo* fluorescent labeling and sensing applications[4,5] may be addressed through the use of freestanding silicon nanocrystals (Si-NCs). While studies have indicated several factors beyond the NC core can contribute significantly to cytotoxic effects (*e.g.*, surface charge[6] or hydrodynamic radius[4]), it has been suggested that nanostructured Si can indeed be biologically compatible.[1,6−11]

We have developed a synthetic method for Si-NCs embedded in SiO_2, from the thermal processing of hydrogen silsesquioxane (HSQ) under reducing atmosphere.[12,13] This synthesis is scalable to tangible quantities of composite material with narrow size distribution and a well-defined oxide interface. These Si-NCs exhibit size-dependent PL shifts consistent with quantum confinement effects, with emission maxima spanning the visible and near-IR spectral region. The origin of luminescence in these materials was recently studied using X-ray excited optical luminescence (XEOL), showing evidence for quantum confinement effects influencing the PL.[14]

A key step in the development of applications utilizing freestanding Si-NCs is the tailoring of surface groups to render the NCs dispersible in the desired medium and protect the surface against oxidation. This is commonly achieved through realization of a chemically active surface (*e.g.*, Si−Br, Si−Cl, Si−OH, Si−H) that allows for further modification.[15] These chemically active nanostructured Si surfaces rapidly oxidize under ambient conditions, resulting in undesirable changes to their solution dispersibility and PL properties. Oxidation under ambient conditions impacts the desired electronic and optical properties of Si-NCs, even at low levels. For instance, Wolkin and co-workers have proposed the formation of a silanone (Si═O) surface defect on an otherwise hydride-terminated surface leads to localized midgap states, leading to a red-shift in the PL of Si-NCs below *ca.* 3 nm.[16] As well, Eyre and co-workers predicted other oxide species such as silanol (Si−OH) and bridging oxide (Si−O−Si) groups can affect Si-NC PL, leading to red- or blue-shifts with strong dependence on the surface species and degree of oxidation.[17]

Of the methods reported for surface modification, hydrofluoric acid (HF) etching

***Address correspondence to jveinot@ualberta.ca.**

Received for review May 11, 2010 and accepted July 13, 2010.

Published online July 27, 2010. 10.1021/nn101022b

to realize surface hydride species and subsequent hydrosilylation with alkenes and alkynes offers several advantages for tailoring the NC surface.[15,18−20] HF etching of Si-NCs prepared from HSQ removes the oxide matrix and reduces the NC size, shifting the PL emission maxima to higher energy, from the near IR to the visible spectral regions.[12] Hydrosilylation can be driven under extremely mild conditions, with minimal reaction byproducts and toleration of a range of functional groups. The Si−C surface bonds formed are both thermodynamically and kinetically robust, limiting oxidative surface degradation under a variety of damaging conditions;[15,19,21,22] for freestanding Si-NCs, hydrosilylation helps protect the PL under conditions where hydride-terminated NCs are rapidly oxidized.[23,24] Importantly, for many applications such as *in vivo* labeling which require highly luminescent, water-soluble Si-NCs, hydrosilylation is a convenient method to produce colloidal Si-NCs in aqueous environments, either by way of covalent attachment of a polar species (*e.g.*, carboxylic acid,[2,25,26] amine,[3,6,23,27] alcohol[28] and polyethylene glycol[29]) on the distal end of the alkene or through the use of a dispersing agent such as a phospholipid micelle,[7,30] polymer,[31] or cosolvent.[32]

Many reports of Si-NC surface modification demonstrate a shift in the optical properties of Si-NCs (*i.e.*, emission maxima and high quantum yield) during the modification procedures. Both blue- and red-shifts have been reported depending on the starting NC diameter and method of functionalization.[33] In particular, reports on the origin of blue PL from Si-NCs have differed depending on the synthetic technique and functionalization procedure used. For example, the groups of Swihart and Kortshagen have shown oxidative treatment of orange emitting alkyl-capped Si-NCs can "shut off" the orange emission with the concurrent appearance of a new emission centered in the blue.[20,34] Conversely, the groups of Kauzlarich, Zuilhof, and Tilley have demonstrated solution-phase syntheses of Si-NCs with subsequent Pt-catalyzed hydrosilylation that give blue PL.[3,31,35]

Many reports of red- to green-emitting Si-NCs have shown an indirect bandgap with characteristic long (μs to ms) radiative lifetimes, implying the electronic structure of nanostructured Si is intimately related to its parent bulk properties. Brus suggested the dominant factor that gives rise to efficient PL from Si-NCs is the removal of efficient nonradiative relaxation mechanisms such as Auger and deep trap processes, rather than a transition to a pseudodirect bandgap.[36] Yet, some reports of blue-emitting Si-NCs have shown fast (ns) radiative lifetimes.[3,20,35]

The reported differences in the optical response of Si-NCs functionalized by hydrosilylation could be due to a wide range of variables, including the methods used to prepare and purify the Si-NCs (*e.g.*, starting NC diameter, inherent size distribution, byproduct impurities), differences in the reaction conditions utilized (*e.g.*, thermal, photochemical, or metal-catalyzed reaction), or differences in postfunctionalization treatment. Critical evaluation of the impact of hydrosilylation on the electronic and optical properties is thus challenging.

Photochemically initiated hydrosilylation merits unique consideration for photoluminescent Si materials. Photochemical and thermal hydrosilylation of bulk surfaces has been generally regarded to follow a free-radical mechanism *via* homolytic cleavage of a hydride bond (requiring *ca.* 3.5 eV).[19,37] However, Stewart and Buriak have proposed a secondary mechanism specific to nanostructured, photoluminescent Si that operates *via* the absorption of low energy light to form excitons (*i.e.*, below the energy required for hydride cleavage).[38,39] This "white light" method occurs under extremely mild conditions and is compatible with a range of alkene substrates. The main stipulation for this proposed mechanism is the nanostructure remains photoluminescent during the reaction in order to facilitate a long-lived exciton that can drive the irreversible Si−C formation process. While radical quenching species were observed to have no impact on the functionalization, energy- and charge-transfer species that quenched the PL resulted in a low degree of surface coverage. This was noted in particular for alkenes and alkynes that quench nanostructured Si PL, such as phenylacetylene and vinylferrocene.

Furthermore, recent controversy has emerged over the mechanism of photochemical hydrosilylation on Si surfaces, in particular the initiation step. This has led to a number of new proposed mechanisms, including exciton-mediated[40,41] and photoemission[42] processes for bulk Si surfaces. These proposed mechanisms hint there may be a complex relationship among the wavelength of irradiation, the alkene or alkyne species attached, and the quantum size effects in determining the mechanism of hydrosilylation in preparing functionalized Si surfaces.

Here we present an investigation of the impact of photochemical hydrosilylation on the optical and electronic properties of Si-NCs prepared from HSQ, using a 365 nm light source to initiate functionalization. We have chosen to study photochemical hydrosilylation using this wavelength for several reasons. First, these reactions can be carried out using commercially available UV-LEDs, which offer relatively high power and low heat output, and may present a "gentler" method for surface modification in comparison to other light sources (*e.g.*, Hg bulb for deep-UV light). As well, some alkene and alkyne substrates of interest absorb strongly at deep-UV wavelengths, leading to undesired decomposition and polymerization byproducts. Conversely, some substrates are expected to quench hydrosilylation *via* the proposed exciton-mediated mechanism; a near-UV source might be able to initiate functionalization through both the free-radical and exciton-mediated mechanism, giving a wider range of acces-

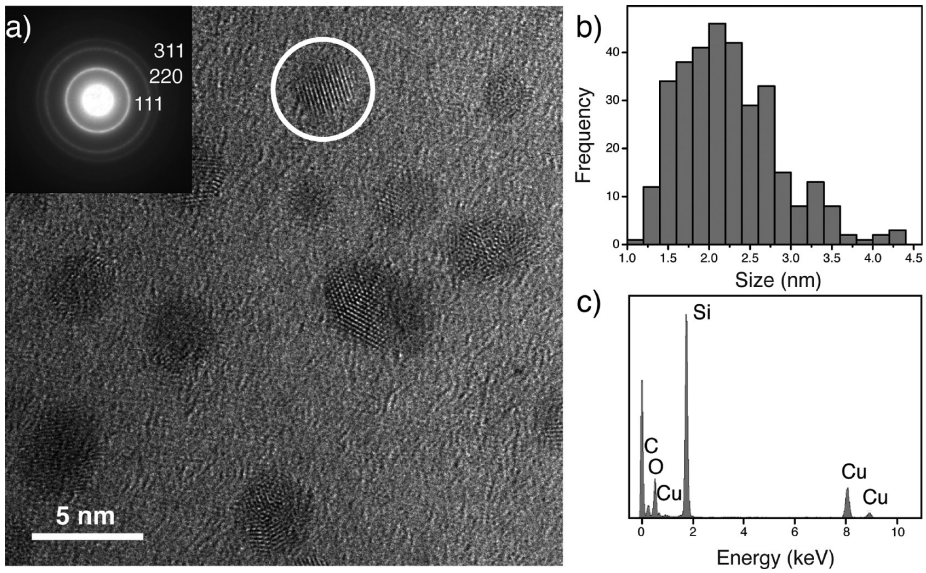

Figure 1. HRTEM (A), SAED (inset), EDS (B), and size distribution information (C) (2.3 ± 0.6 nm, n = 328) of Si-NCs functionalized with 1-hexene (etched for 1 h, initially red emitting). The lattice fringes of the circled nanocrystal a d-spacing of 1.9 Å, matching the 220 plane of crystalline Si.

sible alkene and alkynes. Finally, near-UV light can also efficiently stimulate PL in these materials, as Si-NCs can absorb this spectral range by means of a direct-gap transition, giving a significantly larger absorption coefficient than phonon-mediated indirect absorption at energies closer to the Si-NC bandgap.[36,43] This facilitates collection of the PL produced during the reaction, and allows assessment of the impact of the changing surface chemistry on the optical properties.

We have investigated the influence of near-UV initiated hydrosilylation with straight-chain alkenes, which have been studied in the literature for their ability to protect the Si-NC surface from ambient oxidation and its detrimental effects on the PL. As well, we have studied the reaction of Si-NC surfaces with conjugated alkynes with varied electron demand to better understand the interaction between the surface of Si-NCs and PL-quenching species. Better understanding of this interaction could give insight into the nature of the interface between Si-NCs and species such as organic semiconductors.

The materials in the present study were characterized by PL, UV−vis absorption, and Fourier-transform infrared (FTIR) spectroscopies, dynamic light scattering (DLS), thermogravimetric analysis (TGA), high-resolution transmission electron microscopy (HRTEM), selected electron area diffraction (SAED), and energy dispersive X-ray spectroscopy (EDS).

RESULTS AND DISCUSSION

Near-UV Hydrosilylation with Model Alkenes/Alkynes. A common goal in functionalization of silicon nanostructures is protection of the PL under ambient conditions. As mentioned above, hydrosilylation with straight-chain alkenes imparts stability to Si-NC surfaces; however, some authors have observed shifts in the optical response during the functionalization process. Near-UV hydrosilylation was studied using the model molecules 1-hexene, styrene, and 1-hexyne and compared to a control sample where hydride-terminated Si-NCs were irradiated by the light source in toluene in the absence of any alkene/alkyne. Si-NCs with initial red PL, etched with HF for 1 h (λ_{max} *ca.* 700 nm, referred in the text as "red" Si-NCs) and initial green/yellow PL, etched with HF for 2 h (λ_{max} *ca.* 580-600 nm, referred in the text as "red" Si-NCs) were compared.

Figure 1 shows a representative HRTEM of red Si-NCs functionalized with 1-hexene, with a mean size 2.3 ± 0.6 nm (Figure S1 in the Supporting Information shows HRTEM of analogously prepared green Si-NCs with mean size 2.0 ± 0.5 nm). Lattice parameters and selected area electron diffraction were consistent with crystalline Si. EDS indicated the presence of Si, C, and O.

Absorption, PL, and PL excitation (PLE) spectra of red Si-NCs after functionalization with styrene are shown in Figure 2. The Si-NCs exhibit continuous and relatively featureless absorption, characteristic of an indirect band gap. Extrapolation to the *x*-axis gives an approximate band gap of 2.6 eV. The PLE spectrum shows a broad feature centered at approximately 4 eV. These features can be related to the calculated absorption spectrum of bulk Si, which has an indirect region from 1.1 to 3.4 eV and direct-gap absorption from 3.4 to 4.4 eV.[36,44] Absorption studies of other nanostructured Si materials show similar spectra to those presented here, and suggest the direct-gap transition broadens and slightly red-shifts at the nanoscale.[36,43,44] Thus, a rationalization for the choice of a near-UV exciting wavelength for photochemical hydrosilylation can be inferred. In the exciton-mediated mechanism proposed by Stewart and Buriak, the functionalization process is driven by surface-localized excitons created through

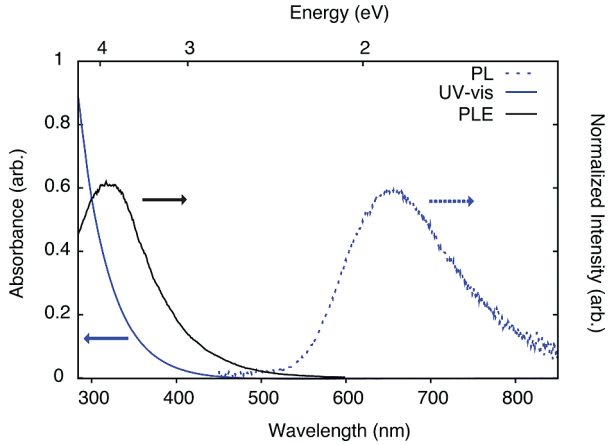

Figure 2. Absorption (blue solid line), PLE (black solid line, monitoring at 640 nm), and PL (blue dashed line, λ_{ex} = 365 nm) of styrene-functionalized red Si-NCs after hydrosilylation in toluene.

photoabsorption. The correlation of direct-gap absorption with a significant increase in intensity in the PLE spectrum implies this absorption route leads to more efficient exciton formation over indirect-gap absorption, which requires a phonon. Therefore, more excitons are created which can facilitate Si−C bond formation.

FTIR spectroscopy was used to qualitatively study the degree of Si−C bond formation, shown in Figure 3 (FTIR spectra of additional alkyne-functionalized Si-NCs are shown in Figure S2). This bond formation process is most evident in the observation of a Si−C═C stretch at 1600 cm^{-1} in Si-NCs functionalized with 1-hexyne. This stretch is characteristic of a silyl-bonded alkene, being red-shifted by *ca.* 40 cm^{-1} in comparison to aliphatic alkenes;[38] furthermore, the absence of sp C−H and C≡C stretches at *ca.* 3300 and 2120 cm^{-1} suggests no starting material remains.

Immediately following HF etching, the hydride-terminated Si-NCs exhibit SiH_x (x = 1−3) stretching bands at *ca.* 2100 cm^{-1} and scissoring bands at *ca.* 910 cm^{-1} with little or no oxide present. Upon functionalization, a broad SiH_x stretching band is typically observed at reduced intensity in qualitative comparison to other features, consistent with other reports that coverage of Si surfaces by hydrosilylation is limited by steric interactions between surface-bonded moieties.[19] Partial oxidation of SiH_x surfaces has been observed to shift the hydride stretching band to higher energy, with a characteristic stretch at 2250 cm^{-1} for O_3Si-H species indicating high levels of surface oxidation. Conversely, formation of Si−C bonds has been predicted to shift the frequency to lower energy.[45] The broad feature centered at 2100 cm^{-1} in the present samples is consistent with Si−C bond formation without the formation of the heavily oxidized O_3Si-H species. Surface oxidation is observed in functionalized samples through the observation of Si−O−Si and Si−OH bands at *ca.* 1100 and 3400 cm^{-1}, respectively. One disadvantage of using aqueous HF etching to control NC size is the difficulty in eliminating any trace water from the reaction mixture; photochemical oxidation of the Si surface *via* water-related radical species is one possible source of this oxidation.[46] Furthermore, while efforts were made to minimize exposure of the functionalized surfaces after reaction where possible, the propensity of surface hydride species to oxidize under ambient conditions makes it challenging to fully rule out the impact of ambient exposure on the oxide-related features in the FTIR spectra.

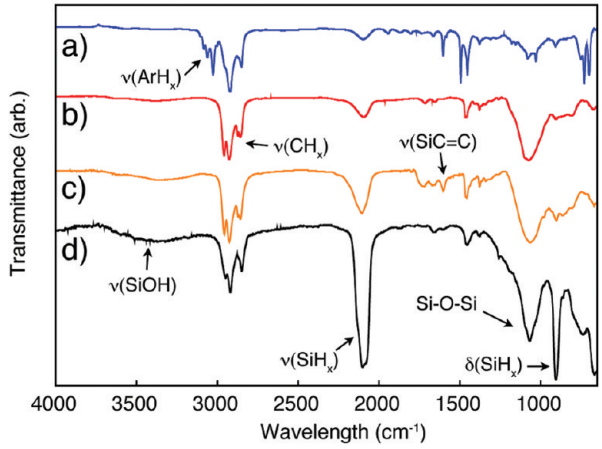

Figure 3. FTIR spectra of red Si-NCs functionalized with (a) styrene, (b) 1-hexene, and (c) 1-hexyne. A control sample irradiated in the absence of any alkene/alkyne (d) is also shown. Spectra are normalized to the alkyl stretching band at *ca.* 2950 cm^{-1}.

FTIR spectra of the alkene-functionalized Si-NCs exhibit alkyl stretching features at *ca.* 2900 cm^{-1} (CH_2 and CH_3 ν stretching) and *ca.* 1460 and 1380 cm^{-1} (CH δ deformation) consistent with alkyl species grafted during hydrosilylation. Styrene functionalized Si-NCs also show aromatic C−H stretching bands at *ca.* 3070−3010 cm^{-1} and combination and overtone bands at 2000−1650 cm^{-1}. An FTIR spectrum of the control Si-NC sample also shows prominent alkyl stretching, which could arise from physisorbed organic species. Thus, quantitative integration of these signals in comparison to the Si−H features would give an artificially high degree of surface coverage. The Si−C ν stretching band, which would directly confirm surface hydrosilylation, is obscured in the fingerprint region.[45,47] However, qualitative comparison of the hydride to alkyl stretching regions show the styrene and 1-hexene functionalized samples have reduced hydride intensity, consistent with a higher degree of surface coverage.

Functionalization with near-UV hydrosilylation was also qualitatively evaluated based on the quality of dispersions (photo shown in Figure 4). Functionalization yielded Si-NCs that gave clear dispersions that could easily pass through a 0.45 μm filter, whereas the control sample was cloudy and rapidly precipitated out of solution. As well, DLS measurements (see Figure S3 in Supporting Information) of functionalized Si-NCs in toluene gave hydrodynamic radii in the range of 8−15

nm. DLS of the control sample showed agglomerates with hydrodynamic radii of ca. 100 nm. This is consistent with the replacement of surface hydrides with alkyl/alkenyl groups through near-UV functionalization, increasing particle−solvent affinity and decreasing particle agglomeration. Hydrodynamic radii of other functionalized NCs with 2−3 nm diameters in toluene have been shown to be in a similar range to the present observations;[48] NC hydrodynamic radii have also been shown to be dependent on the NC core, surface capping agent and concentration effects.

TGA (see Figure S4 in Supporting Information) was used to qualitatively evaluate surface coverage of red Si-NCs (etched for 1 h). This has some advantages over other methods such as integration of FTIR band intensities[38] for freestanding systems where reproducible integration of IR bands is challenging.[18]

TGA of red Si-NCs functionalized with styrene and 1-hexene showed weight losses of *ca.* 70 and 55%, respectively; taking into account the molecular weight of the alkenes, this could suggest similar degrees of surface coverage. These results are very close to reported weight losses for deep-UV hydrosilylation of Si-NCs with these alkenes.[18] TGA of green functionalized Si-NCs with these alkenes (not shown) gave similar weight losses. In comparison, TGA of 1-hexyne-functionalized Si-NCs showed a reduced weight loss of 30%. As will be discussed below, functionalization with other alkynes that quench the Si-NC PL also translates to a reduced weight loss, in the range of 20−25%.

These observations can be explained in the context of the free-radical and exciton-mediated mechanisms proposed for photochemical hydrosilylation on nanostructured Si surfaces. If the exciton-mediated pathway is dominant at the exciting wavelength of 365 nm (possibly due to direct-gap absorption increasing the cross-section for exciton formation), reaction with alkenes or alkynes that preserve the PL should lead to a higher degree of surface coverage and hence greater TGA weight loss. Quenching substrates could only react by the free-radical route. This is also supported qualitatively by the relative intensity of Si−H features in the FTIR spectra of functionalized samples (*vide supra*). Surface alkenyl groups formed by reaction with 1-hexyne or phenylacetylene have been observed to partially or fully quench Si-NC PL, also consistent with our PL data during the reaction described below.[38] However, we note that a complicating factor in interpreting these TGA results is the potential for partial decomposition of surface alkenyl groups during heating, which may limit the overall weight loss and skew the observed trend. A recent study of alkyl-capped Ge-NCs has shown the alkyl groups decompose during heating, forming carbonaceous residues.[49] Ongoing TGA-MS experiments are being conducted in our lab to better understand the thermal decomposition of surface bound species.

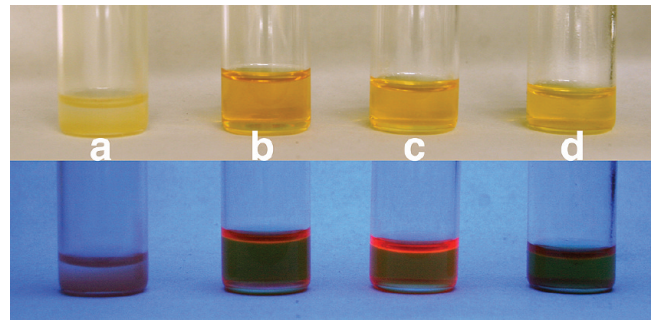

Figure 4. Toluene dispersions of Si-NCs under ambient (top) and UV irradiation (bottom): functionalization with (a) control sample (no alkene present), (b) styrene, (c) 1-hexene, and (d) phenylacetylene.

Since near-UV light can initiate exciton formation through direct gap absorption (and thus enable the hydrosilylation process to occur by the exciton-mediated pathway), it can efficiently stimulate PL in these materials. This enables observation of the PL as the surface chemistry changes during the reaction, making *in situ* comparisons of emission maxima and intensity possible. This direct measurement also eliminates any ambient oxidation during postreaction analysis that might complicate comparisons. Figure 5 shows *in situ* PL measurements made throughout the functionalization of Si-NCs. Initially red-emitting samples functionalized with styrene, 1-hexene, and 1-hexyne initially exhibit a decrease in PL intensity, followed by a blue-shift of *ca.* 40 nm and increase in intensity. The rate at which these changes occur is dependent upon the alkene used. Functionalization with styrene and 1-hexene resulted in an increase to *ca.* 160−180% of the original PL intensity, whereas reaction with 1-hexyne gave approximately 95% of the original intensity. In comparison, the control sample (which was irradiated in the absence of any alkene/alkyne) did not show any shift in the PL maxima, and a decrease in intensity to *ca.* 75% of the original PL. The QY of the styrene-functionalized red Si-NCs was found to be 4.6%, comparable to similar Si-NCs functionalized by deep-UV hydrosilylation.[34] While this QY is lower than some of the highest reports in the literature,[50] one possible way to increase this would be extended annealing under H_2/Ar of the Si-NC/SiO_2 composites before etching, which has been shown to reduce nonradiative defects in these materials.[13]

Functionalization of green Si-NCs showed a decrease in intensity during the reaction; reaction with styrene reduced the intensity to *ca.* 35% of the original, whereas 1-hexene reduced it to *ca.* 70%. This loss in intensity was accompanied by a red-shift of *ca.* 40−60 nm. The green control sample showed rapid, near-complete PL quenching. While FTIR spectra and TGA of the functionalized green samples did not suggest appreciable differences in surface coverage between the styrene and 1-hexene functionalized samples, the lower PL intensity observed for the sty-

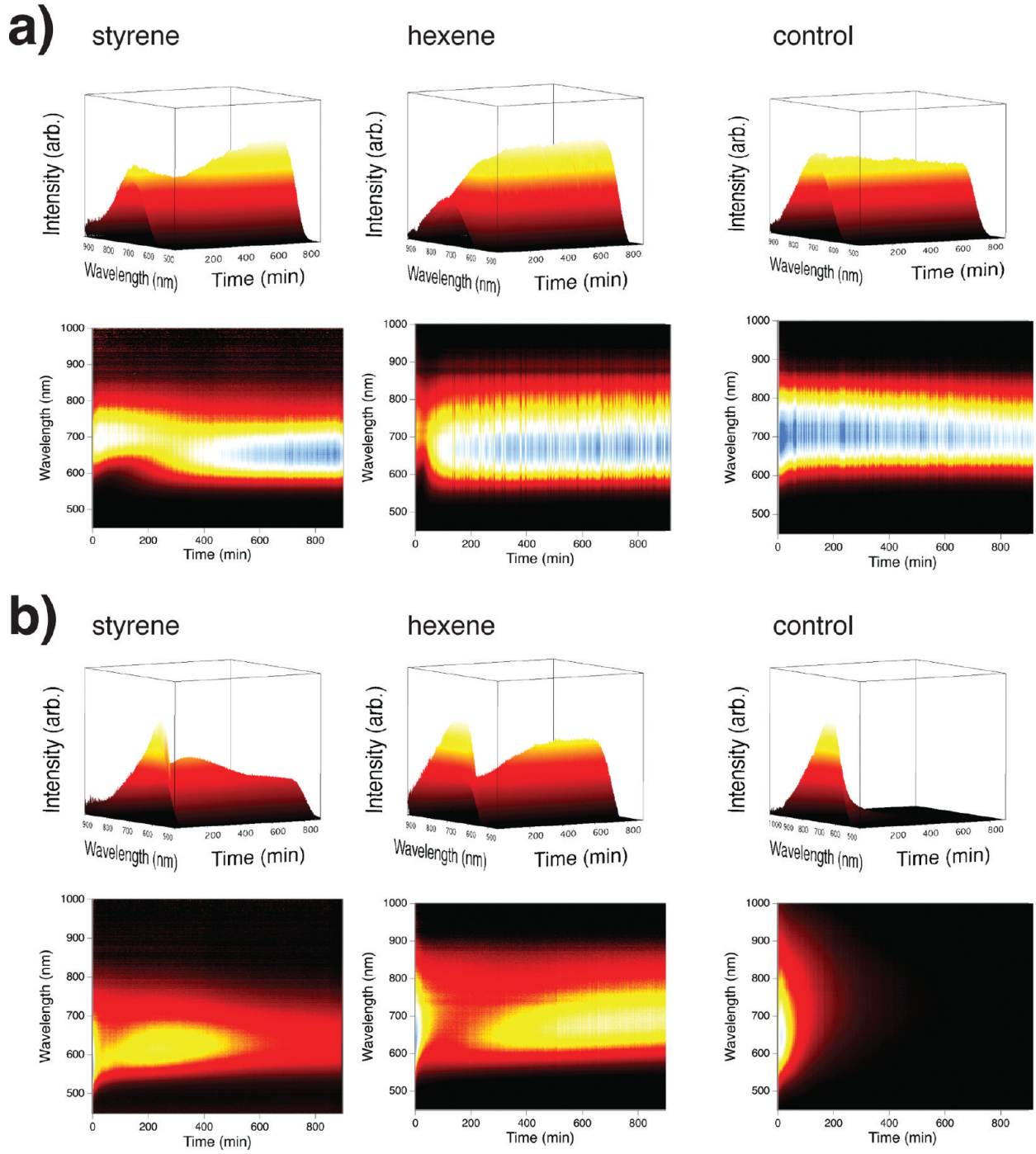

Figure 5. ***In situ*** **PL measurements of (a) red and (b) green Si-NCs during reaction with styrene and 1-hexene, in comparison to control samples. Oblique (top) and top-down (bottom) views of the spectra are shown.**

rene sample may result from poorer packing of the alkyl surface groups due to greater solvent interactions, resulting in a surface more susceptible to oxidation during reaction.[51]

The observed changes in intensity for these samples are a product of the intrinsic quantum yield and scattering by the dispersion as it changes from cloudy to clear. As the surface chemistry changes during the functionalization, it could introduce a transitive reaction intermediate (such as surface radicals or cations produced as part of the free radical or exciton-mediated hydrosilylation mechanisms) or oxide-related surface states that could quench or trap NC excited states. Furthermore, as aggregates of nonfunctionalized Si-NCs disperse into the solvent, more light reaches the spectrometer, resulting in an apparent increase in PL intensity.

Similar PL shifts have been observed for other nanostructured Si materials, and have been generally attributed to the influence of surface oxidation. The model of silanone defects proposed by Wolkin *et al.* has three

size regimes relevant to the trapping of Si-NC excited states by metastable silanone (Si═O) species, formed during the oxidation of the Si surface; this species is thought to trap either electrons or both electrons and holes depending upon the size of the NC. This results in band to midgap state or entirely "trapped exciton" transitions, respectively, and hence a resulting red-shift.[16] This model is in agreement with our observations of PL from functionalized green Si-NCs; as the Si-NC size decreases as a result of HF etching, the conduction and valence band states "open up," allowing the midgap state formed by oxidation during the near-UV irradiation to alter the luminescence. The rapid decrease of PL from the control PL sample, and overall decrease in intensity of the functionalized green samples suggests that oxidation also introduces nonradiative trap states, consistent with other reports showing a decrease in QY as a result of oxidation.[50]

However, this does not fully explain the blue-shift observed for the styrene and 1-hexene functionalized red Si-NCs. Pi *et al*. observed a blue-shift of *ca*. 30 nm for Si-NCs with a mixture of Si−H, Si−C, Si−F, and Si-CF_x surface species, and attributed it to a quantum-confined related blue-shift thought to arise from oxidation reducing the Si-NC diameter.[20,52] However this does not appear to be the case in the present system, as PL from the control sample irradiated without alkene, which also showed signs of surface oxidation, did not shift appreciably, suggesting the red Si-NCs lie outside the size regime where silanone defects could affect the PL. Similar observations of this blue-shift have been made by Gupta *et al*. for deep-UV hydrosilylation;[33] however, an explanation was not proposed.

One possible explanation for this behavior could be the involvement of surface states other than the oxide-related ones extensively studied in the literature. The so-called "smart confinement" model of Si-NC luminescence first suggested that strained surface and/or dangling bonds (*e.g.*, Si═Si dimers) could form trapping midgap states, resulting in a red-shift away from a purely band-mediated transition.[53,54] It has also been suggested that dangling bonds formed as a result of surface reconstruction can quench the Si-NC PL through the formation of deep midgap states. Recently, the role of shallow-trapping midgap states formed by a suboxide surface species has also been demonstrated in the PL of oxide-embedded Si-NCs by high-field magneto-PL.[55] While it is a considerable challenge to conclusively determine the structure of the (possibly metastable) surface species responsible for this behavior (analogous to the highly reactive Si═Si dimer first proposed), the concept of a shallow-trap with as-of-yet unknown structure could explain the blue-shift in PL observed. If trapping states were formed by surface reconstruction of the hydride-terminated Si-NCs during HF etching, this could result in a surface-mediated transition red-shifted from the purely quantum confined bandgap. Evidence for strained surface bonding can be found in the inhomogeneously broadened Si−H stretching region of these NCs, with linewidths significantly larger than that of hydride-terminated bulk Si.[53] Changing the surface chemistry to Si−C species during hydrosilylation could alter the structure of these traps and remove their influence on the PL. This would cause a blue-shift and increase in quantum yield; qualitatively this is consistent with the present observations. Further efforts to test this hypothesis and better understand the impact of hydrosilylation on the Si-NC PL are ongoing in our group.

Near-UV Hydrosilylation with Conjugated Alkynes. In addition to preservation of the Si-NC PL and tailoring particle dispersibility in a range of solvents, functionalization by hydrosilylation may also be of interest for the synthesis and study of hybrid organic/inorganic composite materials where the optical and electronic properties (*e.g.*, charge separation and carrier mobility) are tunable based on the interaction of the Si-NCs and host polymer matrix at the NC surface. One family of model organic semiconductors that has received attention is π-conjugated species tethered to the Si surface with covalent alkyl/alkenyl linkages *via* hydrosilylation. For example, hydrosilylation of bulk Si with phenylacetylene, creating a surface styrenyl group, has been suggested as a route to well-defined organic/inorganic junctions,[37] and has been noted to enhance interfacial conductivity over bare hydride-terminated surfaces.[56,57] Other conjugated species such as thiophenes have been studied, for example in the preparation of covalently bound polythiophenes.[58,59] In contrast, hydrosilylation of nanostructured Si surfaces with π-conjugated aromatics has not been as fully investigated for their resulting optical and electronic properties. As noted above, in the proposed exciton mechanism for photochemical hydrosilylation, conjugated alkynes did not react appreciably under white light irradiation. This was attributed to the ability of these species to effectively trap excitons required for nucleophilic attack from the alkyne, the first step required in the mechanism, supported by low levels of surface group incorporation (<1% based on FTIR integration) and a significant reduction in PL intensity.

However, the present 365 nm source is at the threshold of energy required for homolytic cleavage of surface hydrides indentified in the free-radical mechanism. While lower energy "white light" produces a very low degree of coverage, near-UV light might initiate functionalization (*via* the free-radical mechanism) as well as stimulate PL, allowing direct measurement of the impact of these conjugated species during the course of the reaction. Figure 6 shows *in situ* PL of Si-NCs reacted with alkynes phenylacetylene, 4-ethynylanisole, 1-ethynyl-3-fluorobenzene, and 3-ethynylthiophene. These were chosen on the basis of their electron withdrawing/donating ability while being cognizant of any competing side reactions with functional groups (*e.g.*,

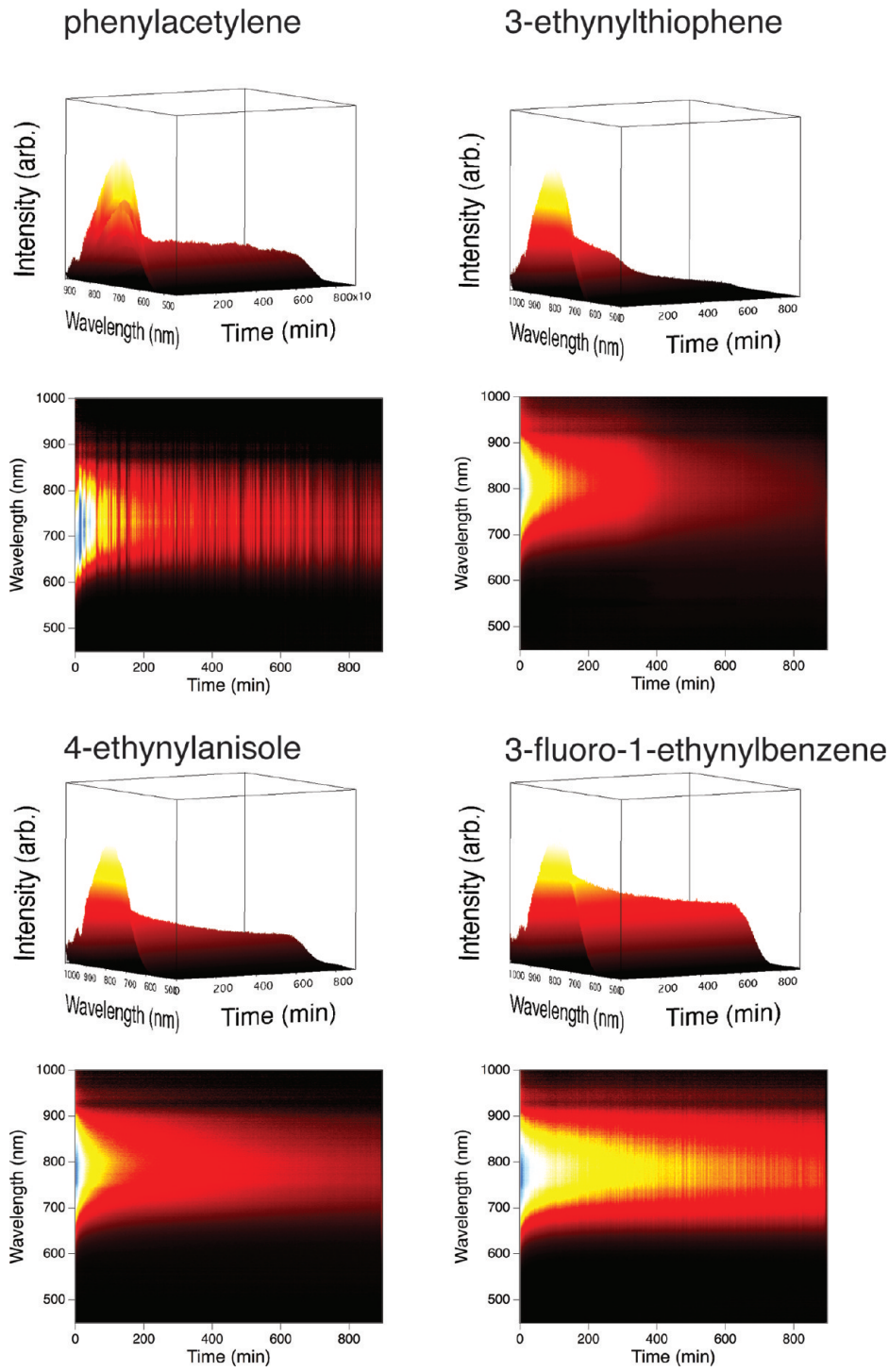

Figure 6. *In situ* PL measurements of red Si-NCs during reaction with (a) phenylacetylene, (b) 3-ethynylthiophene, (c) 4-ethynylanisole, and (d) 1-ethynyl-3-fluorobenzene. Oblique (top) and top-down (bottom) views of the spectra are shown.

amines[60] or bromine groups[61]). The PL decays over the course of the experiment at a rate dependent on the alkyne used; the greater the electron-donating character of the substituent, the faster the rate of PL decay. For example, functionalization with 3-ethynylthiophene gave near complete PL quenching, whereas 1-ethynyl-3-fluorobenzene reduced the Si-NC PL to *ca.* 38% of the original intensity over the course of the reaction. The remaining PL intensity comes from unfunctionalized hydride-terminated NCs, which are separated from the reaction mixture during workup as they quickly precipitate out of dispersion during the first centrifugation; FTIR of this precipitate (not shown) gave predominately Si−H and Si−O−Si features at *ca.* 2100 and 1100 cm^{-1}, respectively, with very small amounts of alkyl features.

This trend in reactivity was also supported qualitatively by FTIR of the Si-NCs after purification (Supporting Information, Figure S2). Si-NCs functionalized with

alkynes of greater electron-withdrawing character show an increase in the intensity of hydride- and oxide-related bands compared to alkyl stretching features; this implies a lower degree of incorporation of the alkenyl surface groups. In the context that the free-radical mechanism that we propose is dominant here, these observations suggest the surface silyl radicals are electrophilic. This is consistent with the established facile reactivity toward olefins of radicals of this type.[22] Greater electron density in the alkyne would lead to a faster rate of reaction, higher degree of surface coverage, and hence faster rate of PL quenching. A similar trend was noted in the deep UV hydrosilylation of Si-NCs with alkenes.[18] We note that in the photoemission mechanism for hydrosilylation of bulk surfaces with deep UV light proposed by Wang *et al*. the rate of reaction and therefore degree of surface coverage depended on the affinity of the alkene to accept a photoelectron from the bulk Si surface.[42] The observed trend of electron-donating groups increasing the rate of reaction in the present system seems to contradict this observation; this may suggest the photoemission mechanism does not hold for these alkyne substrates and on nanostructured Si surfaces. It is important to emphasize the challenge in comparing hydrosilylation reactivity between systems with different alkenes (and purity), initiating wavelength, and different quantum size effects (*i.e.*, bulk surface *versus* nanostructured). Other recent reports of hydrosilylation have also suggested factors intrinsic to the experimental design may influence reactivity, including the observations of self-assembly in the dark at room temperature,[62] and reaction catalyzed by surface groups on the glassware commonly used to carry out these reactions.[63] Further study is required in this area to better understand hydrosilylation of Si-NCs and optimize surface coverage.

Quenching of nanostructured Si PL has been reported for other conjugated species, both physisorbed[60] and covalently bound.[38,64] However, the mechanism of quenching has remained unclear. In the present system, all of the alkynes gave functionalized Si-NCs with no PL detectable to the naked eye following particle purification, suggesting the differences observed in the *in situ* PL measurements arises from differences in hydrosilylation reactivity. This could be due to the formation of a deep trap in the Si-NC bandgap, as changing the electron demand of the surface group did not turn on the Si-NC PL (and thus enable the exciton mediated mechanism for hydrosilylation). Further experimental and computational studies to understand this quenching are ongoing.

CONCLUSIONS

We have studied photochemical hydrosilylation of silicon nanocrystals (Si-NCs) with alkene and alkynes using a near-UV light source. The impact of the changing surface chemistry on the photoluminescence (PL) and the relevant mechanism of hydrosilylation was dependent on the NC size and structure of the alkene/alkyne. For Si-NCs with initial green/yellow (580−600 nm) PL reacted with model alkenes, styrene, and 1-hexene, a red-shift and decrease in PL intensity was observed, consistent with the formation of midgap oxide-related states. Hydrosilylation of Si-NCs with initial red (680−700 nm) PL gave an increase in intensity, possibly related to the production of well-dispersed particles with less scattering or an increase in the intrinsic quantum yield, as well as a blue-shift. A qualitative model based on the formation of Si−C surface species was proposed to account for the shift. As well, hydrosilylation was studied using conjugated alkynes; this reaction quenched the Si-NC PL at a rate dependent on the electron-donating ability of the alkene. These results were rationalized in the context of the free-radical and exciton-mediated mechanisms postulated for hydrosilylation of nanostructured Si surfaces. These model alkynes may be interesting in the integration of Si-NCs into hybrid composite materials with tunable optical and electronic properties.

MATERIALS AND METHODS

Materials. HSQ (Dow Corning, trade name FOx-17, sold as a solution in methyl isobutyl ketone and toluene), 49% hydrofluoric acid (HF, J.T. Baker, electronics grade), and 95% ethanol (Sigma-Aldrich) were used as received. High-purity water (18.2 MΩ/cm) was obtained from a Barnstead Nanopure Diamond purification system. Toluene and methanol were obtained from Sigma Aldrich as reagent grade. All alkenes and alkynes (styrene, 1-hexene, phenylacetylene, 4-ethnylanisole, 1-ethynyl-3-fluorobenzene, 3-ethynylthiophene) were purchased from Sigma Aldrich as the highest purity available and were purified before use by passing over neutral alumina to remove inhibitor and/or peroxide impurities.[38]

Synthesis and Etching of Si-NCs. Oxide-embedded Si-NC composites were prepared as previously described.[12] In brief, solvent was removed from a solution of HSQ under vacuum to yield a white solid. This was heated at 18 °C/min to 1100 °C in a Lindberg/Blue furnace, and annealing for 1 h under a flowing 5% H_2/95% Ar atmosphere yielded a glassy brown product. Previous X-ray diffraction and TEM characterization is in agreement with the formation of *ca.* 3 nm diamond structured Si-NCs encapsulated in an silica matrix.

To produce freestanding hydride-terminated Si-NCs, an oxide-embedded composite was etched using solutions of HF as previously described.[12] To 1 g of mechanically ground composite in a Teflon beaker equipped with a stir bar was added 30 mL of a 1:1:1 solution of HF/ethanol/water (**Caution!** HF is highly dangerous and must be handled with extreme care). After 1 h of stirring, the dispersion changed color from brown to yellow, and gave Si-NCs with initial red PL (*ca.* 700 nm, referred to as "red" Si-NCs in the text). Etching for 2 h gave Si-NCs with initial green/yellow PL (*ca.* 580−600 nm, referred to as "green" Si-NCs in the text). Liberated hydride-terminated Si-NCs were extracted with two 25 mL aliquots of toluene.

Functionalization. Immediately after etching, the organic extracts were combined and added to a Schlenk flask equipped with a quartz insert, a stir bar, and 32.5 mmol freshly purified alkene/alkyne. The flask was placed on a Schlenk line under an argon atmosphere and degassed by three freeze−pump−thaw cycles.

Hydrosilylation functionalization was initiated using a near-UV LED light source. The light source consisted of two 365 nm LEDs (Nichia, model NCSU033A) operated at 4.5 V, mounted at 180° to each other on a water-cooled bracket. The flask was thoroughly wrapped in aluminum foil and irradiation commenced for 15 h. The Si-NC emission was monitored during functionalization as described below.

Following functionalization, the Si-NCs were transferred into test tubes and centrifuged at 3000 rpm to remove any aggregated or unreacted material. The supernatant was filtered through a 0.45 μm PTFE filter and transferred to a round-bottom flask equipped with a stir bar. Excess solvent and alkene/alkyne were removed under vacuum on a Schlenk line. The sample was redispersed in a minimum of toluene, transferred into centrifuge tubes, and precipitated *via* the addition of methanol followed by centrifugation in a high speed centrifuge at 17 000 rpm. The supernatant was decanted, and the redispersion, precipitation, and centrifugation steps were repeated 2 times.

Material Characterization and Instrumentation. FTIR spectra were collected using a Nicolet Magna 750 IR spectrometer on drop-cast films. HRTEM was performed at the Brockhouse Institute for Materials Research (BIMR) at McMaster University using a Titan^3 G2 60−300 TEM operating at 300 kV. SAED and EDS were performed using a JEOL-2010 field-emission gun operating at 200 kV. TGA was performed using a Perkin-Elmer Pyris 1 TGA. Sample in a Pt pan were heated under N_2 from 20 to 900 °C at a rate of 10 °C/min. DLS measurements were performed using a Malvern Zetasizer Nano S series dynamic light scatterer. Dilute sample in toluene were equilibrated to 25 °C and refiltered through a 0.45 μm PTFE syringe filter prior to analysis. Samples sets (of 10) were scanned three times. During the functionalization, the Si-NC PL was collected at 3 min intervals through an optical fiber connected to an Ocean Optics USB2000 spectrometer. The spectrometer's spectral response was normalized using a blackbody radiator. Quantum yield (QY) measurements were done by a relative method (described in detail in the Supporting Information) on toluene dispersions of styrene-functionalized Si-NCs in quartz cuvettes, using a Cary 400 UV−vis spectrometer and a Cary Eclipse fluorescence spectrophotometer.

Acknowledgment. The authors acknowledge funding from the Natural Sciences and Engineering Research Council of Canada (NSERC), Canada Foundation for Innovation (CFI), Alberta Science and Research Investment Program (ASRIP), Alberta Ingenuity and University of Alberta Department of Chemistry. C.W. Moffat is thanked for assistance with FTIR, TGA, and UV−vis characterization. C. Andrei and the Brockhouse Institute for Materials Research are thanked for HRTEM imaging. J. Rodríguez, M. Dang, M. Johnson, S. Regli, R. Clark, E.J. Henderson, C.M. Hessel and B. Benoit are thanked for useful discussions.

Supporting Information Available: Detailed procedure for quantum yield measurements, HRTEM of green-etched Si functionalized with 1-hexene, FTIR of alkyne-functionalized Si-NCs, TGA weight loss curves of alkene/alkyne functionalized Si-NCs, and DLS measurements. This material is available free of charge *via* the Internet at http://pubs.acs.org.

REFERENCES AND NOTES

1. Park, J.; Gu, L.; von Maltzahn, G.; Ruoslahti, E.; Bhatia, S. N.; Sailor, M. J. Biodegradable Luminescent Porous Silicon Nanoparticles for *in Vivo* Applications. *Nat. Mater.* **2009**, *8*, 331–336.
2. Li, Z. F.; Ruckenstein, E. Water-Soluble Poly(acrylic acid) Grafted Luminescent Silicon Nanoparticles and Their Use as Fluorescent Biological Staining Labels. *Nano Lett.* **2004**, *4*, 1463–1467.
3. Warner, J. H.; Hoshino, A.; Yamamoto, K.; Tilley, R. D. Water-Soluble Photoluminescent Silicon Quantum Dots. *Angew. Chem., Int. Ed.* **2005**, *44*, 4550–4554.
4. Soo Choi, H.; Liu, W.; Misra, P.; Tanaka, E.; Zimmer, J. P.; Itty Ipe, B.; Bawendi, M. G.; Frangioni, J. V. Renal Clearance of Quantum Dots. *Nat. Biotechnol.* **2007**, *25*, 1165–1170.
5. Lewinski, N.; Colvin, V.; Drezek, R. Cytotoxicity of Nanoparticles. *Small* **2008**, *4*, 26–49.
6. Ruizendaal, L.; Bhattacharjee, S.; Pournazari, K.; Rosso-Vasic, M.; De Haan, L. H. J.; Alink, G. M.; Marcelis, A. T. M.; Zuilhof, H. Synthesis and Cytotoxicity of Silicon Nanoparticles with Covalently Attached Organic Monolayers. *Nanotoxicology* **2009**, *3*, 339–347.
7. Erogbogbo, F.; Yong, K. -.; Roy, I.; Xu, G. X.; Prasad, P. N.; Swihart, M. T. Biocompatible Luminescent Silicon Quantum Dots for Imaging of Cancer Cells. *ACS Nano* **2008**, *2*, 873–878.
8. Alsharif, N. H.; Berger, C. E. M.; Varanasi, S. S.; Chao, Y.; Horrocks, B. R.; Datta, H. K. Alkyl-Capped Silicon Nanocrystals Lack Cytotoxicity and Have Enhanced Intracellular Accumulation in Malignant Cells *via* Cholesterol-Dependent Endocytosis. *Small* **2009**, *5*, 221–228.
9. Bayliss, S. C.; Heald, R.; Fletcher, D. I.; Buckberry, L. D. Culture of Mammalian Cells on Nanostructured Silicon. *Adv. Mater.* **1999**, *11*, 318–321.
10. Nagesha, D. K.; Whitehead, M. A.; Coffer, J. L. Biorelevant Calcification and Noncytotoxic Behavior in Silicon Nanowires. *Adv. Mater.* **2005**, *17*, 921–924.
11. Low, S. P.; Voelcker, N. H.; Canham, L. T.; Williams, K. A. The Biocompatibility of Porous Silicon in Tissues of the Eye. *Biomaterials* **2009**, *30*, 2873–2880.
12. Hessel, C. M.; Henderson, E. J.; Veinot, J. G. C. Hydrogen Silsesquioxane: A Molecular Precursor for Nanocrystalline Si-SiO_2 Composites and Freestanding Hydride-Surface-Terminated Silicon Nanoparticles. *Chem. Mater.* **2006**, *18*, 6139–6146.
13. Hessel, C. M.; Henderson, E. J.; Veinot, J. G. C. An Investigation of the Formation and Growth of Oxide-Embedded Silicon Nanocrystals in Hydrogen Silsesquioxane-Derived Nanocomposites. *J. Phys. Chem. C* **2007**, *111*, 6956–6961.
14. Hessel, C. M.; Henderson, E. J.; Kelly, J. A.; Cavell, R. G.; Sham, T. K.; Veinot, J. G. C. Origin of Luminescence from Silicon Nanocrystals: A Near Edge X-ray Absorption Fine Structure (NEXAFS) and X-ray Excited Optical Luminescence (XEOL) Study of Oxide-Embedded and Free-Standing Systems. *J. Phys. Chem. C* **2008**, *112*, 14247–14254.
15. Veinot, J. G. C. Synthesis, Surface Functionalization, and Properties of Freestanding Silicon Nanocrystals. *Chem. Commun.* **2006**, 4160–4168.
16. Wolkin, M. V.; Jorne, J.; Fauchet, P. M.; Allan, G.; Delerue, C. Electronic States and Luminescence in Porous Silicon Quantum Dots: The Role of Oxygen. *Phys. Rev. Lett.* **1999**, *82*, 197–200.
17. Eyre, R. J.; Goss, J. P.; Briddon, P. R. Effect of Progressive Oxidation on the Optical Properties of Small Silicon Quantum Dots: A Computational Study. *Phys. Rev. B: Condens. Matter* **2008**, *77*, 245407.
18. Hua, F.; Swihart, M. T.; Ruckenstein, E. Efficient Surface Grafting of Luminescent Silicon Quantum Dots by Photoinitiated Hydrosilylation. *Langmuir* **2005**, *21*, 6054–6062.
19. Buriak, J. M. Organometallic Chemistry on Silicon and Germanium Surfaces. *Chem. Rev.* **2002**, *102*, 1271–1308.
20. Pi, X. D.; Liptak, R. W.; Deneen Nowak, J.; Wells, N. P.; Carter, C. B.; Campbell, S. A.; Kortshagen, U. Air-Stable Full-Visible-Spectrum Emission from Silicon Nanocrystals Synthesized by an All-Gas-Phase Plasma Approach. *Nanotechnology* **2008**, *19*, 245603.
21. Ciampi, S.; Harper, J. B.; Gooding, J. J. Wet Chemical Routes to the Assembly of Organic Monolayers on Silicon Surfaces *via* the Formation of Si−C Bonds: Surface Preparation, Passivation and Functionalization. *Chem. Soc. Rev.* **2010**, *39*, 2158–2183.

22. Chatgilialoglu, C.; Timokhin, V. I. Silyl Radicals in Chemical Synthesis. In *Advances in Organometallic Chemistry*; Academic Press: Oxford, U.K., 2008; Vol. 57, pp 117−181.
23. Rosso-Vasic, M.; Spruijt, E.; Popoví, Z.; Overgaag, K.; Van Lagen, B.; Grandidier, B.; Vanmaekelbergh, D.; Domínguez-Gutiérrez, D.; De Cola, L.; Zuilhof, H. Amine-Terminated Silicon Nanoparticles: Synthesis, Optical Properties and Their Use in Bioimaging. *J. Mater. Chem.* **2009**, *19*, 5926–5933.
24. Li, X.; He, Y.; Swihart, M. T. Surface Functionalization of Silicon Nanoparticles Produced by Laser-Driven Pyrolysis of Silane Followed by HF-HNO_3 Etching. *Langmuir* **2004**, *20*, 4720–4727.
25. Rogozhina, E. V.; Eckhoff, D. A.; Gratton, E.; Braun, P. V. Carboxyl Functionalization of Ultrasmall Luminescent Silicon Nanoparticles through Thermal Hydrosilylation. *J. Mater. Chem.* **2006**, *16*, 1421–1430.
26. Sato, S.; Swihart, M. T. Propionic-Acid-Terminated Silicon Nanoparticles: Synthesis and Optical Characterization. *Chem. Mater.* **2006**, *18*, 4083–4088.
27. Rosso-Vasic, M.; DeCola, L.; Zuilhof, H. Efficient Energy Transfer between Silicon Nanoparticles and a Ru−Polypyridine Complex. *J. Phys. Chem. C* **2009**, *113*, 2235–2240.
28. Shiohara, A.; Hanada, S.; Prabakar, S.; Fujioka, K.; Lim, T. H.; Yamamoto, K.; Northcote, P. T.; Tilley, R. D. Chemical Reactions on Surface Molecules Attached to Silicon Quantum Dots. *J. Am. Chem. Soc.* **2010**, *132*, 248–253.
29. Sudeep, P. K.; Page, Z.; Emrick, T. PEGylated Silicon Nanoparticles: Synthesis and Characterization. *Chem. Commun.* **2008**, 6126–6127.
30. Goller, B.; Polisski, S.; Wiggers, H.; Kovalev, D. Silicon Nanocrystals Dispersed in Water: Photosensitizers for Molecular Oxygen. *Appl. Phys. Lett.* **2010**, *96*, 211901.
31. Zhang, X.; Neiner, D.; Wang, S.; Louie, A. Y.; Kauzlarich, S. M. A New Solution Route to Hydrogen-Terminated Silicon Nanoparticles: Synthesis, Functionalization, and Water Stability. *Nanotechnology* **2007**, *18*, 095601.
32. Dickinson, F. M.; Alsop, T. A.; Al-Sharif, N.; Berger, C. E. M.; Datta, H. K.; Sïller, L.; Chao, Y.; Tuite, E. M.; Houlton, A.; Horrocks, B. R. Dispersions of Alkyl-Capped Silicon Nanocrystals in Aqueous Media: Photoluminescence and Ageing. *Analyst* **2008**, *133*, 1573–1580.
33. Gupta, A.; Swihart, M. T.; Wiggers, H. Luminescent Colloidal Dispersion of Silicon Quantum Dots from Microwave Plasma Synthesis: Exploring the Photoluminescence Behavior Across the Visible Spectrum. *Adv. Funct. Mater.* **2009**, *19*, 696–703.
34. Hua, F.; Erogbogbo, F.; Swihart, M. T.; Ruckenstein, E. Organically Capped Silicon Nanoparticles with Blue Photoluminescence Prepared by Hydrosilylation Followed by Oxidation. *Langmuir* **2006**, *22*, 4363–4370.
35. Rosso-Vasic, M.; Spruijt, E.; Van Lagen, B.; De Cola, L.; Zuilhof, H. Alkyl-Functionalized Oxide-Free Silicon Nanoparticles: Synthesis and Optical Properties. *Small* **2008**, *4*, 1835–1841.
36. Brus, L. E.; Szajowski, P. F.; Wilson, W. L.; Harris, T. D.; Schuppler, S.; Citrin, P. H. Electronic Spectroscopy and Photophysics of Si Nanocrystals: Relationship to Bulk c-Si and Porous Si. *J. Am. Chem. Soc.* **1995**, *117*, 2915–2922.
37. Cicero, R. L.; Linford, M. R.; Chidsey, C. E. D. Photoreactivity of Unsaturated Compounds with Hydrogen-Terminated Silicon(111). *Langmuir* **2000**, *16*, 5688–5695.
38. Stewart, M. P.; Buriak, J. M. Exciton-Mediated Hydrosilylation on Photoluminescent Nanocrystalline Silicon. *J. Am. Chem. Soc.* **2001**, *123*, 7821–7830.
39. Reboredo, F. A.; Schwegler, E.; Galli, G. Optically Activated Functionalization Reactions in Si Quantum Dots. *J. Am. Chem. Soc.* **2003**, *125*, 15243–15249.
40. Sun, Q.-Y.; De Smet, L. C. P. M.; Van Lagen, B.; Giesbers, M.; Thüne, P. C.; Van Engelenburg, J.; De Wolf, F. A.; Zuilhof, H.; Sudhölter, E. J. R. Covalently Attached Monolayers on Crystalline Hydrogen-Terminated Silicon: Extremely Mild Attachment by Visible Light. *J. Am. Chem. Soc.* **2005**, *127*, 2514–2523.
41. De Smet, L. C. P. M.; Pukin, A. V.; Sun, Q.-Y.; Eves, B. J.; Lopinski, G. P.; Visser, G. M.; Zuilhof, H.; Sudhölter, E. J. R. Visible-Light Attachment of SiC Linked Functionalized Organic Monolayers on Silicon Surfaces. *Appl. Surf. Sci.* **2005**, *252*, 24–30.
42. Wang, X.; Ruther, R. E.; Streifer, J. A.; Hamers, R. J. UV-Induced Grafting of Alkenes to Silicon Surfaces: Photoemission *versus* Excitons. *J. Am. Chem. Soc.* **2010**, *132*, 4048–4049.
43. Holmes, J. D.; Ziegler, K. J.; Doty, R. C.; Pell, L. E.; Johnston, K. P.; Korgel, B. A. Highly Luminescent Silicon Nanocrystals with Discrete Optical Transitions. *J. Am. Chem. Soc.* **2001**, *123*, 3743–3748.
44. Ben-Chorin, M.; Averboukh, B.; Kovalev, D.; Polisski, G.; Koch, F. Influence of Quantum Confinement on the Critical Points of the Band Structure of Si. *Phys. Rev. Lett.* **1996**, *77*, 763–766.
45. Bateman, J. E.; Eagling, R. D.; Horrocks, B. R.; Houlton, A. A Deuterium Labeling, FTIR, and *ab Initio* Investigation of the Solution-Phase Thermal Reactions of Alcohols and Alkenes with Hydrogen-Terminated Silicon Surfaces. *J. Phys. Chem. B* **2000**, *104*, 5557–5565.
46. Bahruji, H.; Bowker, M.; Davies, P. R. Photoactivated Reaction of Water with Silicon Nanoparticles. *Int. J. Hydrogen Energy* **2009**, *34*, 8504–8510.
47. Canaria, C. A.; Lees, I. N.; Wun, A. W.; Miskelly, G. M.; Sailor, M. J. Characterization of the Carbon-Silicon Stretch in Methylated Porous Silicon—Observation of an Anomalous Isotope Shift in the FTIR Spectrum. *Inorg. Chem. Commun.* **2002**, *5*, 560–564.
48. Pons, T.; Uyeda, H. T.; Medintz, I. L.; Mattoussi, H. Hydrodynamic Dimensions, Electrophoretic Mobility, and Stability of Hydrophilic Quantum Dots. *J. Phys. Chem. B* **2006**, *110*, 20308–20316.
49. Holman, Z. C.; Kortshagen, U. R. Solution-Processed Germanium Nanocrystal Thin Films as Materials for Low-Cost Optical and Electronic Devices. *Langmuir* **2009**, *25*, 11883–11889.
50. Jurbergs, D.; Rogojina, E.; Mangolini, L.; Kortshagen, U. Silicon Nanocrystals with Ensemble Quantum Yields Exceeding 60%. *Appl. Phys. Lett.* **2006**, *88*, 233116.
51. Sieval, A. B.; Vleeming, V.; Zuilhof, H.; Sudhölter, E. J. R. Improved Method for the Preparation of Organic Monolayers of 1-Alkenes on Hydrogen-Terminated Silicon Surfaces. *Langmuir* **1999**, *15*, 8288–8291.
52. Ledoux, G.; Guillois, O.; Porterat, D.; Reynaud, C.; Huisken, F.; Kohn, B.; Paillard, V. Photoluminescence Properties of Silicon Nanocrystals as a Function of their Size. *Phys. Rev. B: Condens. Matter* **2000**, *62*, 15942–15951.
53. Koch, F.; Petrova-Koch, V.; Muschik, T. The Luminescence of Porous Si: The Case for the Surface State Mechanism. *J. Lumin.* **1993**, *57*, 271–281.
54. Nayfeh, M. H.; Rigakis, N.; Yamani, Z. Photoexcitation of Si−Si Surface States in Nanocrystallites. *Phys. Rev. B: Condens. Matter* **1997**, *56*, 2079–2084.
55. Godefroo, S.; Hayne, M.; Jivanescu, M.; Stesmans, A.; Zacharias, M.; Lebedev, O. I.; Van Tendeloo, G.; Moshchalkov, V. V. Classification and Control of the Origin of Photoluminescence from Si Nanocrystals. *Nat. Nanotechnol.* **2008**, *3*, 174–178.
56. Hiremath, R. K.; Mulimani, B. G.; Rabinal, M. K.; Khazi, I. M. Electrical Characterization of a Phenylacetylene-Modified Silicon Surface *via* Mercury Probe. *J. Phys.: Condens. Matter* **2007**, *19*, 446003.
57. Saito, N.; Hayashi, K.; Sugimura, H.; Takai, O. Microstructured π-Conjugated Organic Monolayer Covalently Attached to Silicon. *Langmuir* **2003**, *19*, 10632–10634.
58. Fabre, B.; Lopinski, G. P.; Wayner, D. D. M. Photoelectrochemical Generation of Electronically Conducting Polymer-Based Hybrid Junctions on Modified Si(111). Surfaces. *J. Phys. Chem. B* **2003**, *107*, 14326–14335.
59. Sathyapalan, A.; Ng, S. C.; Lohani, A.; Ong, T. T.; Chen, H.; Zhang, S.; Lam, Y. M.; Mhaisalkar, S. G. Novel Self Assembled Monolayers of Allyl Phenyl Thiophene Ether as

Potential Dielectric Material for Organic Thin Film Transistors. *Thin Solid Films* **2008**, *516*, 5645–5648.
60. Song, J. H.; Sailor, M. J. Quenching of Photoluminescence from Porous Silicon by Aromatic Molecules. *J. Am. Chem. Soc.* **1997**, *119*, 7381–7385.
61. Wang, D.; Buriak, J. M. Trapping Silicon Surface-Based Radicals. *Langmuir* **2006**, *22*, 6214–6221.
62. Scheres, L.; Arafat, A.; Zuilhof, H. Self-Assembly of High-Quality Covalently Bound Organic Monolayers Onto Silicon. *Langmuir* **2007**, *23*, 8343–8346.
63. Mischki, T. K.; Lopinski, G. P.; Wayner, D. D. M. Evidence for Initiation of Thermal Reactions of Alkenes with Hydrogen-Terminated Silicon by Surface-Catalyzed Thermal Decomposition of the Reactant. *Langmuir* **2009**, *25*, 5626–5630.
64. Song, J. H.; Sailor, M. J. Functionalization of Nanocrystalline Porous Silicon Surfaces with Aryllithium Reagents: Formation of Silicon−Carbon Bonds by Cleavage of Silicon−Silicon Bonds. *J. Am. Chem. Soc.* **1998**, *120*, 2376–2381.